



Size distributions of nitrated phenols in winter at a coastal site in north China and the impacts from primary sources and secondary formation

Yiheng Liang, Xinfeng Wang*, Shuwei Dong, Zhiyi Liu, Jiangshan Mu, Chunying Lu, Jun Zhang, Min Li, Likun Xue, Wenxing Wang

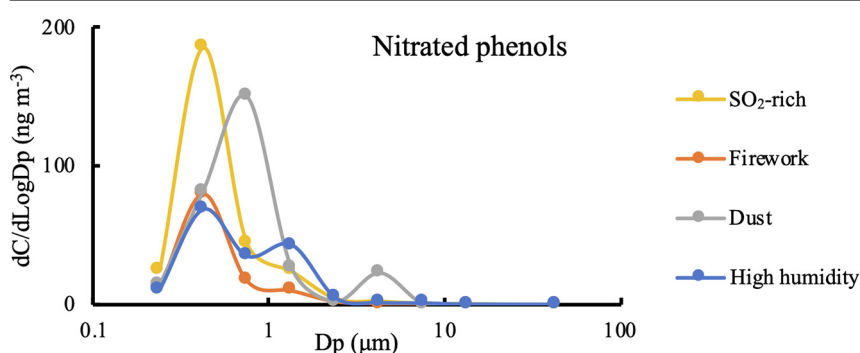
Environment Research Institute, Shandong University, Qingdao, 266237, China



HIGHLIGHTS

- Concentrations and size distributions of 11 nitrated phenols (NPs) were presented.
- Primary sources and secondary formation had impacts on size distributions of NPs.
- Coal combustion and fireworks promoted the increases of NPs in condensation mode.
- Dust in the atmosphere caused the heterogeneous formation of NPs in coarse particles.
- High humidity obviously facilitated the aqueous formation of NPs in droplet mode.

GRAPHICAL ABSTRACT



ARTICLE INFO

Article history:

Received 5 November 2019

Received in revised form

26 January 2020

Accepted 14 February 2020

Available online 18 February 2020

Handling Editor: Hongliang Zhang

Keywords:

Nitrated phenols
Size distribution
Secondary formation
Aqueous formation
Coal combustion
Firework

ABSTRACT

Nitrated phenols in particulate matters are among the major components of brown carbon, harm plant growth and human health. To understand the size distributions of nitrated phenols in the polluted coastal region and the factors influencing these distributions, size-resolved particulate matters were collected from a rural site in the coastal city of Qingdao, China, in January 2019, and analyzed for the presence of 11 nitrated phenols. The average concentrations of total nitrated phenols in fine- and coarse-mode particles were 123.6 and 37.2 ng m⁻³, respectively. 4-Nitrophenol was found to be the dominant nitrated phenol, followed by 3-methyl-6-nitrocatechol, 3-methyl-4-nitrophenol, and 4-nitrocatechol. On average, maximum concentrations of nitrated phenols were in condensation-mode particles, whereas a minor concentration peak of nitro-salicylic acids was present in droplet-mode particles. In addition, a minor concentration peak of 4-methyl-2,6-dinitrophenol was noticed in coarse-mode particles. Comparisons of the size distributions under different situations confirmed that both primary emissions and secondary formation had significant effects on the abundances and particle-sizes of nitrated phenols. Coal combustion in residential villages and firework burning during a festival led to a sharp increase of nitrated phenols in condensation-mode particles, whereas dust promoted their heterogeneous formation in coarse-mode particles, and high humidity in the coastal area facilitated their aqueous formation in droplet-mode particles.

© 2020 Elsevier Ltd. All rights reserved.

* Corresponding author.

E-mail address: xinfengwang@sdu.edu.cn (X. Wang).

1. Introduction

Nitrated phenols are nitrogen-containing organic compounds with a benzene ring substituted with at least one nitro (-NO₂) group and a hydroxyl (-OH) group (Yuan et al., 2016). They have been found to occur in the atmosphere (Rubio et al., 2012; Wang et al., 2018a), cloud, fog (Desyaterik et al., 2013; Hofmann et al., 2008), rainwater (Schummer et al., 2009), and even snow (Harrison et al., 2005). Nitrated phenols generally account for a small fraction of particulate organic matters (Wang et al., 2018a). However, they constitute a considerable part of brown carbon (BrC), which substantially contributes to the absorption of UV and visible light and affects the regional climate (Laskin et al., 2015; Yan et al., 2018). Nitrated phenols have also been reported to harm plants and human health (Harrison et al., 2005). To evaluate the effects of nitrated phenols on the climate, ecosystem, and human health, it is crucial to understand their physical and chemical properties in the atmosphere.

Previous studies have shown that the size distributions of nitrated phenols in fine-mode and coarse-mode particles vary with chemical species and are associated with the nitrated phenols' origins. A previous field study on the size distributions of nitrated phenols conducted in urban Shanghai (Li et al., 2016) found that particulate nitrated phenols are mainly distributed in condensation-mode particles (e.g., nitrocatechols) and coarse-mode particles (e.g., nitrophenols and di-nitrophenols). Several primary emission sources of nitrated phenols from particulate matters have been identified in the past decade, such as biomass burning (Chow et al., 2016; Desyaterik et al., 2013; Iinuma et al., 2010; Kahnt et al., 2013; Kitanovski et al., 2012; Li et al., 2016; Mohr et al., 2013; Wang et al., 2017), coal combustion (Lu et al., 2019a; Wang et al., 2018a), vehicle exhaust (Kohler and Heeb, 2003; Lu et al., 2019b; Rubio et al., 2012; Wang et al., 2018a) and other activities. However, the impacts of these primary sources on the size distributions of nitrated phenols remain unclear. In addition, secondary formation has been recognized as an important contributor to particulate nitrated phenols, especially in the hot season and in the rural and remote areas (Harrison et al., 2005; Wang et al., 2018a; Yuan et al., 2016), as the expected primary emissions are insufficient to support the measured amount of particulate nitrated phenols in the ambient air. In addition, the secondary formation of nitrated phenols in different media (i.e., gas, aqueous droplets, or solid particles) usually yields different size-distribution characteristics.

Possible secondary formation pathways of nitrated phenols in the atmosphere have been proposed in numerous studies via laboratory experiments and modeling simulations (Andreozzi et al., 2006; Finewax et al., 2018; Frka et al., 2016; Harrison et al., 2005; Jenkin et al., 2003; Vione et al., 2005; Wang et al., 2019; Yuan et al., 2016). 4-Nitrophenol (4NP), one of the most abundant nitrated phenols in the atmosphere, can form in the presence of OH radicals or NO₃ radicals in the participation of NO₂ in the gas phase (Harrison et al., 2005; Kowalczyk et al., 2015; Saccon et al., 2013; Wang et al., 2018b, 2019). In addition, 4-nitrophenol serves as an important intermediate in the secondary formation of other nitrated phenols. In the presence of radicals and NO₂, 4-nitrophenol can be further oxidized to 2,4-dinitrophenol (2,4DNP) in the gas phase (Harrison et al., 2005; Vione et al., 2005) and 4-nitrocatechol (4NC) can be produced from catechol in the gas phase (Finewax et al., 2018). Due to their relatively low volatilities, only a fraction of the nitrated phenols generated in the gas phase partition into the particle phase via condensation or uptake on the pre-existing fine or coarse particles or droplets (Wang et al., 2018a; Yuan et al., 2016). In addition, methyl-nitrocatechols, such as 3-methyl-5-nitrocatechol, 3-methyl-4-nitrocatechol, and 3-methyl-6-

nitrocatechol (3M6NC), can be formed by the nitration of methylcatechol in the presence of NO₂ in the aqueous phase, e.g., within small droplets or the liquid layer on the particle surface (Frka et al., 2016). Likewise, in the presence of HNO₃ or N₂O₅, salicylic acid is nitrated to 5-nitro-salicylic acid (5NSA) and 3-nitro-salicylic acid (3NSA) in the aqueous phase (Andreozzi et al., 2006; Harrison et al., 2005). Subsequently, 5-nitro-salicylic acid is converted to 2,4-dinitrophenol in the presence of HNO₃ (Andreozzi et al., 2006). To date, the effects of the above formation pathways on the size-distribution characteristics of particulate nitrated phenols in the real atmosphere have not been evaluated.

In this study, we firstly evaluated the concentrations and variation patterns of nitrated phenols in size-resolved particles. Subsequently, we determined the size distributions of different nitrated phenols and their fractions in different size ranges. Finally, the unique of size-distribution characteristics of nitrated phenols on sulphur dioxide (SO₂)-rich days, during a firework display, during a dust event, and in different humidity levels were compared, and the impacts from primary emission sources and secondary formation were explored.

2. Materials and methods

2.1. Site description

The sampling site was in a coastal area in the north of Qingdao (Aoshanwei, Jimo District), which is located on the east edge of North China (as shown in Fig. 1). The particulate samples were collected at the top of an educational building on the Qingdao Campus of Shandong University (36.36°N, 120.69°E, ~15 m above sea level). The sampling site was surrounded by an educational district and scattered residential districts. As shown in Fig. 2, the Yellow Sea is approximately 500 m east of the site, whereas a low-volume express road is located to ~500 m west of the site. In general, this sampling site is a lightly polluted rural coastal area, which is subjected to a small amount of local anthropogenic emissions from the nearby residential activities and traffic transportation. This light pollution is indicated by the fairly low concentrations of trace gases, e.g., on average 4.9-ppb SO₂ and 24.3-ppb nitrogen oxides (NO_x) during the sampling period.

2.2. Size-resolved sample collection

Size-resolved particulate samples were collected using a Micro-Orifice Uniform Deposition Impactor (MOUDI, MSP, USA) at a flow rate of 30 L min⁻¹. Particulate matters were sampled on quartz fiber filters (Pall Corporation, USA) with a diameter of 47 mm and were divided into nine size ranges, namely 0.18–0.32 μm, 0.32–0.56 μm, 0.56–1 μm, 1–1.8 μm, 1.8–3.2 μm, 3.2–5.6 μm, 5.6–10 μm, 10–18 μm, and 18–100 μm. Due to the lack of a 2.5-μm cut-point, the diameter of 1.8 μm was chosen to distinguish between the fine and coarse particles. The sampling period lasted from January 11 to February 25, 2019, with a temporary break from February 1 to 15 due to the Chinese Lunar Year holiday. Sixteen sets of samples (154 particulate samples in total) were collected daily or once every 2 days, depending on the pollution situation. In addition, one additional set of blank samples (nine samples in total) was collected after the field sampling experiment. The quartz filters were baked in a furnace at 600 °C for 2 h before sampling, to remove any adsorbed organic compounds. After sampling, the sample filters were stored in a refrigerator at -20 °C until subsequent analysis. During the sampling periods, the concentrations of trace gases, that is, ozone (O₃), SO₂, and NO_x, were simultaneously measured by online trace level analyzers (Thermo Scientific, USA). The PM_{2.5} concentrations were taken from the published data that

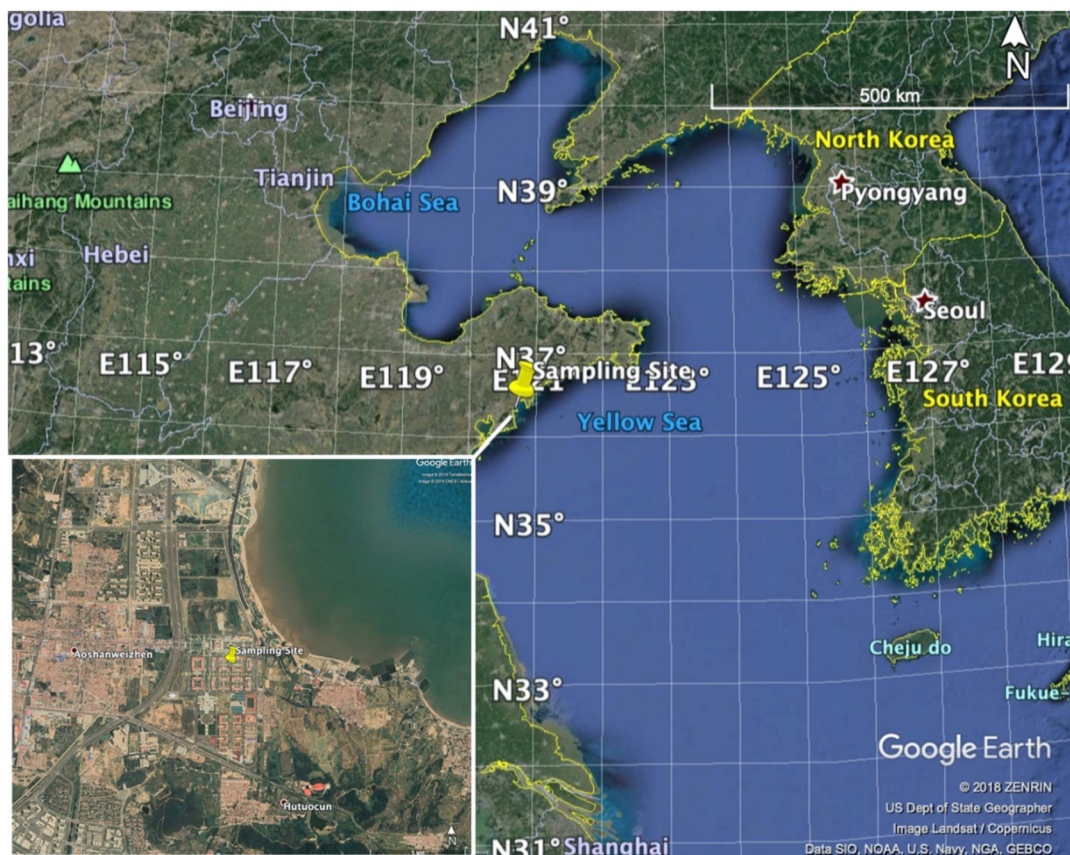


Fig. 1. Maps showing the location of the sampling site on the east edge of North China.

were monitored at the nearest air-quality monitoring station of Yangkou. The data of meteorological parameters, comprising temperature (T), relative humidity (RH), wind direction, and wind speed, were retrieved from the website of Weather Underground (Cloud, 2019).

2.3. Sample treatment and chemical analysis

The filter samples were extracted with 15-mL methanol in a shaker for 40 min and the process was repeated twice. The extracted solution was taken to near-dryness on a rotary evaporator, and the residues were then re-dissolved in 1.5-mL methanol and passed through polytetrafluoroethylene syringe filters (pore size of 0.22 μm). Finally, the filtrates were gently dried under a stream of ultra-high purity nitrogen gently, and the residues were re-dissolved in 300- μL methanol.

The nitrated phenols in sample solutions were analyzed on an Ultimate 3000 ultra-high-performance liquid chromatograph coupled with an ISQ EC mass spectrometer (UHPLC-MS, Thermo Scientific) equipped with an electrospray ionization source. Nitrated phenols were then separated on an Accucore C18 column (150 mm \times 2.1 mm, 3- μm particle size, Thermo Scientific). The mobile phase consisted of eluent A (11% acetonitrile in methanol) and eluent B (11% acetonitrile and 0.1% acetic acid in deionized water). The gradient-elution program started at 90% of eluent B, and gradually decreased to 70% within 19 min. After keeping at 70% for 3 min, the proportion of eluent B increased again to 90% within 8 min.

The channels of eight mass-to-charge (m/z) ratios (138, 152, 154, 166, 168, 182, 183, and 197 amu in the negative ion mode) were

monitored in selective ion monitoring mode. Eleven nitrated phenol species were determined, namely 4-nitrophenol, 3-methyl-4-nitrophenol (3M4NP), 2-methyl-4-nitrophenol (2M4NP), 2,6-dimethyl-4-nitrophenol (2,6DM4NP), 4-nitrocatechol, 4-methyl-5-nitrocatechol (4M5NC), 3-methyl-6-nitrocatechol, 5-nitro-salicylic acid, 3-nitro-salicylic acid, 2,4-dinitrophenol, and 4-methyl-2,6-dinitrophenol (4M2,6DNP). The retention time and MS/MS spectra of standards of these 11 species were used to confirm the identity of the detected species. Five mixed standard solutions in different concentrations were measured to obtain standard curves ($R^2 > 0.99$), which were further used to quantify the contents of nitrated phenols in sample solutions. The average recovery of the nitrated phenols was 94.5%. The standards and reagent chemicals were ordered from Sigma-Aldrich (St. Louis, USA), J&K Chemical (Beijing, China), and Atomax Chemicals (Shenzhen, China).

3. Results and discussion

3.1. Concentrations and variation patterns of nitrated phenols

The average concentrations of the 11 nitrated phenols during the sampling periods are listed in Table 1. As shown in the table, the average total concentrations of nitrated phenols (ΣNPs) in $\text{PM}_{1.8}$ (fine particles) and PM_{10} in rural Qingdao in winter were 123.6 and 150.7 ng m^{-3} , respectively, with an average concentration of 27.1 ng m^{-3} in coarse particles (i.e., $\text{PM}_{1.8-10}$). In fine particles, 4-nitrophenol (on average 37.94 ng m^{-3}) was the most abundant species among the 11 nitrated phenols, followed by 3-methyl-6-nitrocatechol (24.78 ng m^{-3}), 3-methyl-4-nitrophenol (17.21 ng m^{-3}), and 4-nitrocatechol (16.67 ng m^{-3}). In coarse

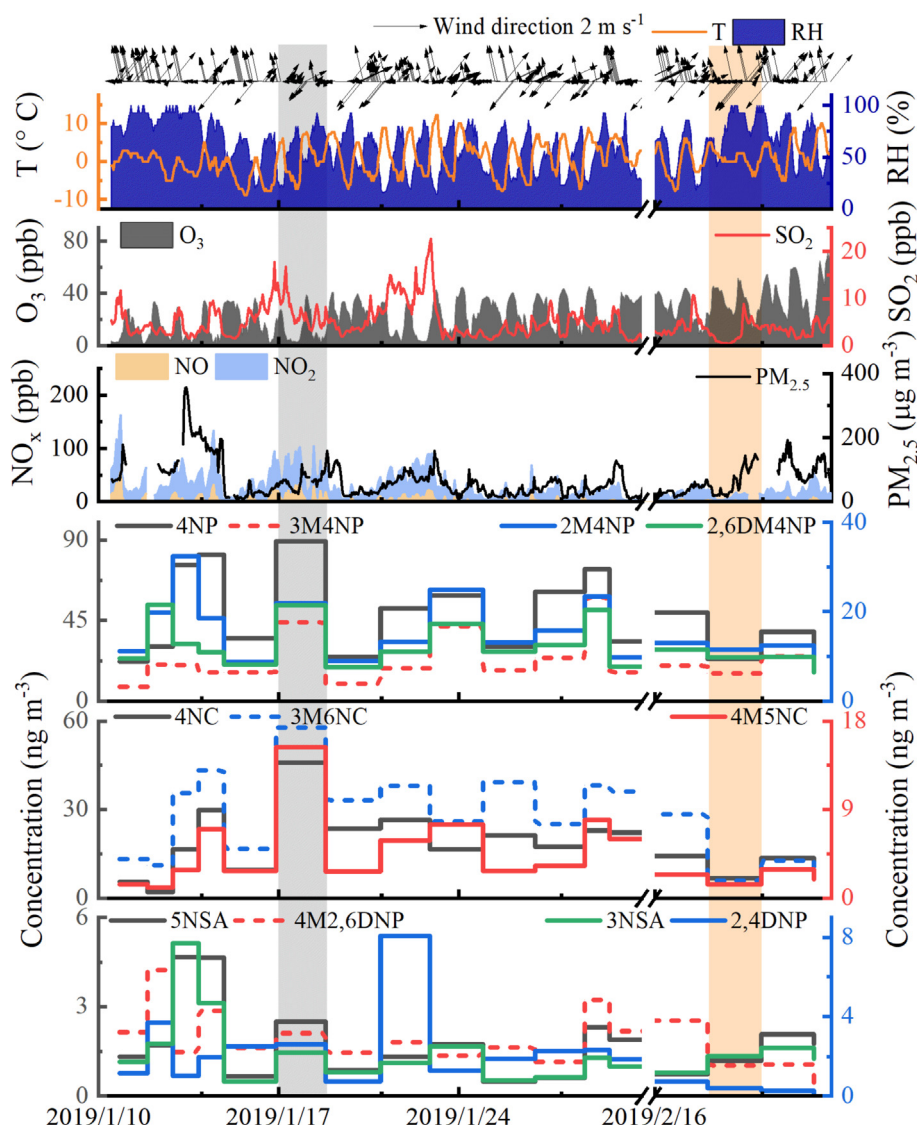


Fig. 2. Time series of the concentrations of nitrated phenols in total suspended particulates and relevant pollutants and meteorological parameters (The grey shade indicates the dust event, and the orange shade indicates the firework event).

Table 1

Average concentrations of nitrated phenols in fine particles and PM_{10} observed in Qingdao in this study and other locations in the literature (unit: $ng\ m^{-3}$).

Location	Type	ΣNPs	4NP	3M4NP	2M4NP	4NC	2,6DM4NP	4M5NC	3M6NC	5NSA	3NSA	2,4DNP	4M2,6DNP	Reference
Rural Qingdao, 2019	$PM_{1.8}$	123.6	37.94	17.21	10.43	16.67	7.86	3.78	24.78	1.46	1.70	0.87	0.91	This study
Urban Jinan, 2013	$PM_{2.5}$	44.58	14.24	4.95	8.14	8.08		2.09	1.01	2.37	3.70			Wang et al. (2018a)
Urban Hong Kong, 2010	$PM_{2.5}$	15.89	3.10	0.27	2	7.86	0.10	2.17	0.39					Chow et al. (2016)
Urban Hong Kong, 2012	$PM_{2.5}$	4.89	1.13	0.07	0.65	2.39	0.01	0.53	0.11					Chow et al. (2016)
Mainz, 2006–2007	PM_3	8.88	2.48			6.40								Zhang et al. (2010)
Rural Qingdao, 2019	PM_{10}	150.7	46.00	21.33	14.37	18.36	11.27	4.49	27.85	1.69	2.07	1.52	1.76	This study
Urban Shanghai, 2013–2015	PM_{10}	363	304			59								Li et al. (2016)
Urban Leibniz, 2014	PM_{10}	16.28	7.09	2.60	3.64		0.65			0.94	1.36			Teich et al. (2017)
Urban Slovenia, 2011	PM_{10}	116.1	1.80	0.61	0.75	75		29	6.20	1.40	1.30	0.02		Kitanovski et al. (2012)
Rural Belgium, 2010	PM_{10}	11.60				11.60								Kahnt et al. (2013)

particles, the most abundant nitrated phenol was 4-nitrophenol ($8.06\ ng\ m^{-3}$), followed by 3-methyl-4-nitrophenol ($4.12\ ng\ m^{-3}$), 2-methyl-4-nitrophenol ($3.94\ ng\ m^{-3}$), and 3-methyl-6-nitrocatechol ($3.07\ ng\ m^{-3}$). Compared with the concentrations of nitrated phenols measured in other locations worldwide in winter (also shown in Table 1), those in Qingdao were found to be

substantially higher, except for those in PM_{10} in Shanghai, which was ascribed to intensive coal and biomass burning. Lu et al. (2019a) reported that the emission profile of nitrated phenols from anthracite combustion exhibited very high concentrations of 4-nitrophenol and 3-methyl-6-nitrocatechol. Consistent with this finding, the high concentrations of 4-nitrophenol and 3-methyl-6-

nitrocatechol observed in our study indicate that the high concentrations of nitrated phenols observed in Qingdao in winter were primarily associated with coal combustion for heating and cooking in nearby residential districts.

The concentrations of nitrated phenols during the sampling periods exhibited large variations. As shown in Fig. 2, the concentrations of individual nitrated phenols in total suspended particulates (PM_{0.18-100}) ranged from 1.80 ng m⁻³ to 48.85 ng m⁻³, and their total concentrations varied from 77.5 ng m⁻³ to 304.9 ng m⁻³. Overall, the variation patterns of the nitrated phenols correlated with each other, especially within the same categories. Notably, the elevated concentrations of most nitrated phenols usually occurred on the days with high concentrations of SO₂ (maximum value > 10 ppb) and NO_x (maximum value > 50 ppb) or high relative humidity (maximum RH > 90%). The maximum concentrations of nitro-salicylic acids occurred on foggy days with very high humidity, or on days with high concentrations of NO_x (maximum value > 50 ppb) and ozone (maximum value > 50 ppb).

Further correlation analyses show that the concentrations of 4-nitrophenol and nitrocatechols in total suspended particles correlated moderately with those of SO₂ and NO, with the linear correlation coefficients (Pearson's *r*) ranging from 0.50 to 0.65 (except for the data on January 21–22). In addition, a moderate correlation was observed between the concentrations of nitro-salicylic acids and relative humidity, with correlation coefficients of 0.57 and 0.67. The moderate correlation coefficients between the concentrations of some nitrated phenols and SO₂ and NO_x further indicate that the elevated concentrations of nitrated phenols in coastal Qingdao in winter were to some extent linked to local coal combustion for heating and cooking. The moderate correlation between the concentrations of nitro-salicylic acids and relative humidity suggests that the aqueous reactions possibly facilitated the formation of nitro-salicylic acids under relatively high humidity in the coastal area.

3.2. Size distributions and compositions of nitrated phenols

Our results show that the 11 nitrated phenols were mostly distributed in fine particles and that different species exhibited difference in size-distribution characteristics. As depicted in Fig. 3, most of the nitrated phenols existed in fine particles, with maximum concentrations in particles < 1.8 μm. Specifically, 4-nitrophenol, methyl- and dimethyl-nitrophenols, 4-nitrocatechol, and methyl-nitrocatechols exhibited a single concentration peak in the size bin of 0.32–0.56 μm (condensation mode). Nitro-salicylic acids showed a major concentration peak in the size bin of 0.32–0.56 μm (condensation mode) and a minor peak in size range of 1.0–1.8 μm (droplet mode). In contrast, 4-methyl-2,6-dinitrophenol appeared with a major concentration peak in the size bin of 0.56–1.0 μm (droplet mode) and a second peak in the size bin of 3.2–5.6 μm (coarse mode). As to 2,4-dinitrophenol, the maximum concentration occurred in the smallest size bin of 0.18–0.32 μm (condensation mode).

The high proportion of nitrated phenols in condensation-mode particles indicates that particulate nitrated phenols measured in rural Qingdao mainly originated from primarily emitted particles and the condensation of gaseous compounds from both primary emission and secondary formation on pre-existing particles. The small and non-negligible concentrations of nitro-salicylic acids and 4-methyl-2,6-dinitrophenol in droplet-mode particles suggest aqueous formation plays a role in their abundances and size distributions. In addition, the elevated concentration of 4-methyl-2,6-dinitrophenol in coarse-mode particles suggests that there was heterogeneous uptake of this gaseous compound on coarse particles (Huang et al., 2019; Li et al., 2011; Luo et al., 2007; Zhang et al., 2003).

The diverse size distributions of nitrated phenols led to different chemical compositions within different size ranges. As shown in Fig. 4, in the smallest size bin of 0.18–0.32 μm (condensation

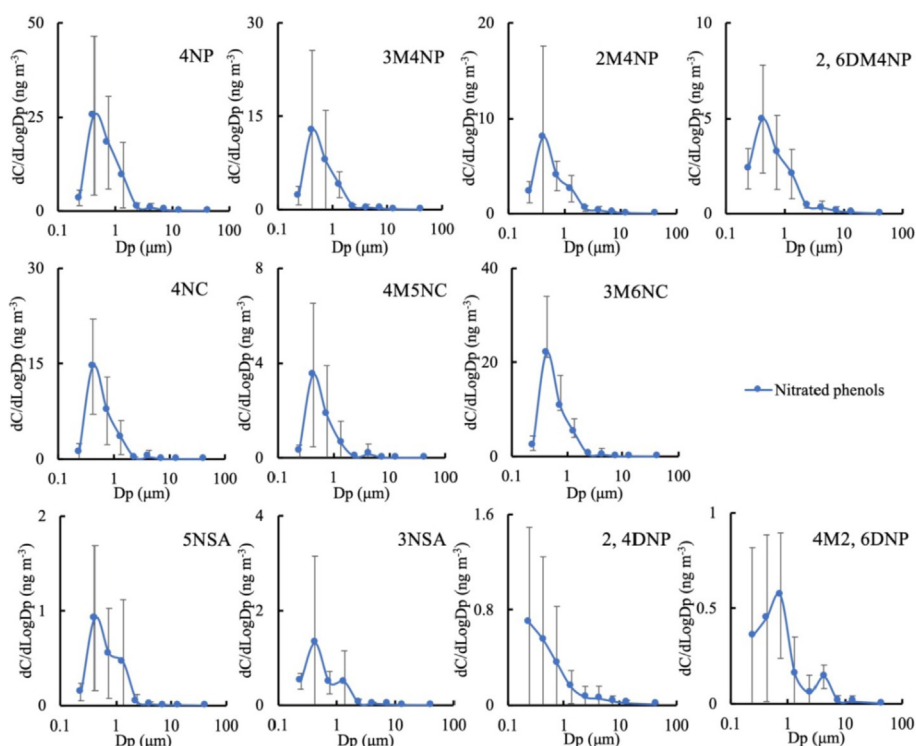


Fig. 3. Averaged size distributions of 11 nitrated phenols in winter in rural Qingdao.

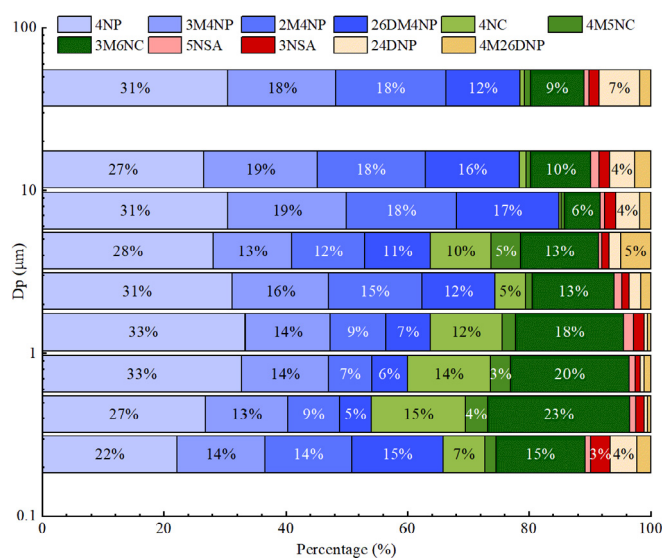


Fig. 4. Averaged fractions of 11 nitrated phenols in different size bins.

mode), 4-nitrophenol (accounting for 22%) was the most abundant of the 11 determined nitrated phenols, followed by 3-methyl-6-nitrocatechol (15%), 2,6-dimethyl-4-nitrophenol (15%), 3-methyl-4-nitrophenol (14%) and 2-methyl-4-nitrophenol (14%). In the condensation-mode particles with size of 0.32–0.56 μm , the proportions of 4-nitrophenol, 3-methyl-6-nitrocatechol, and 4-nitrocatechol increased (27%, 23%, and 15%, respectively), whereas those of 2,6-dimethyl-4-nitrophenol and 2-methyl-4-nitrophenol decreased. As for the droplet-mode particles (0.56–1.8 μm), the proportion of 4-nitrophenol continued to increase (to 33%) and the proportions of 3-methyl-6-nitrocatechol, 3-methyl-4-nitrophenol, and 4-nitrocatechol remained high (18%–20%, 14%, and 12%–14%, respectively). Nevertheless, in coarse-mode particles (1.8–100 μm), the proportions of 2-methyl-4-nitrophenol and 2,6-dimethyl-4-nitrophenol exceeded 10%, whereas those of 3-methyl-6-nitrocatechol and 4-nitrocatechol decreased substantially. In addition, sharp increases were also noted for 2,4-dinitrophenol in 5.6–100 μm and for 4-methyl-2,6-dinitrophenol in 3.2–5.6 μm in the coarse mode.

In general, the relatively high proportions of 4-nitrophenol, methyl-nitrophenols, 4-nitrocatechol, and 3-methyl-6-nitrocatechol in droplet-mode particles indicate that aqueous reactions are important formation pathways for these species. The increased proportions of 2-methyl-4-nitrophenol, 2,6-dimethyl-4-nitrophenol, 2,4-dinitrophenol, and 4-methyl-2,6-dinitrophenol in coarse-mode particles are assumed to be associated with their high saturated vapor pressures, which promoted their heterogeneous uptake on coarse particles (Chim et al., 2017; Shchekin and Podguzova, 2011).

3.3. Size-distribution characteristics when affected by different emission sources

As mentioned previously, particulate nitrated phenols exhibited complex size-distributions and they were highly affected by coal combustion. To understand the effects of primary emissions on the size-distribution characteristics of particulate nitrated phenols, the size distributions of particulate nitrated phenols on the days with obvious coal-combustion emissions, during a firework event, and during a dust event were compared with those on other days (normal samples for comparison, excluding foggy days) (as shown

in Fig. 5). For this comparison, size-resolved samples with SO_2 concentrations >5 ppb were selected to represent the effect of emissions from coal combustion. Fireworks, a common burning activity performed while celebrating festivals in many countries, occurred on February 19 to celebrate the Lantern Festival. In addition, an obvious dust event was observed on January 17–18, that was characterized by elevated PM_{10} concentrations, high $\text{PM}_{10}/\text{PM}_{2.5}$ ratios (>2), and long-range transport of air masses from the Gobi Desert (figure not shown).

As depicted in Fig. 5, during the SO_2 -rich days, nitrated phenols exhibited a sharp concentration peak in condensation-mode particles. The concentrations of most nitrated phenols peaked at 0.32–0.56 μm , except for those of 2,4-dinitrophenol, the maximum concentration of which appeared in the smaller particles (0.18–0.32 μm). In particular, the maximum concentrations of 4-nitrophenol, 4-nitrocatechol, methyl-nitrocatechols, and 2,4-dinitrophenol in condensation-mode particles on SO_2 -rich days were much higher than those in other three situations, indicating the intensive emissions of these species during coal combustion and their rapid formation during the subsequent aging process. The high concentrations of 4-nitrophenol and 3-methyl-6-nitrocatechol (average concentrations >54 ng m^{-3}) were consistent with the reported emission profiles of nitrated phenols from anthracite combustion (Lu et al., 2019a). In addition, increased concentrations of di-nitrophenols were observed in coarse-mode particles, characterized by an apparent concentration peak at 3.2–5.6 μm . This formation of the di-nitrophenols in coarse-mode particles was attributed to the relatively high vapor pressure and moderate acidity, which promoted their heterogeneous uptake on coarse particles (Zhang et al., 2011).

Firework burning is characterized by the production of a large amount of trace gases and particles (Attri et al., 2001; Drewnick et al., 2006; Wang et al., 2014). During the firework event, methyl-nitrophenols, nitro-salicylic acids, 2,4-dinitrophenol, and 4-methyl-2,6-dinitrophenol exhibited a dramatic concentration peak in 0.32–0.56 μm particles. The striking increase in these components indicates the intensive emission and production of nitrated phenols in condensation-mode particles when fireworks were burnt. The directly emitted particulate nitrated phenols and those condensed on pre-existing particles from both primary emissions and secondary formation of gaseous nitrated phenols mostly appeared in condensation-mode particles, and thus caused a sharp concentration peak in 0.32–0.56 μm particles. Notably, the dominant species of 4-nitrophenol, methyl-nitrophenols, and 2,6-dimethyl-4-nitrophenol (all >14 ng m^{-3}) observed from firework burning were some different from those observed from biomass burning (dominated by 4-nitrocatechol and methyl-nitrocatechols) (Wang et al., 2017), coal combustion (dominated by 4-nitrophenol and 3-methyl-6-nitrocatechol, or 4-nitrocatechol and methyl-nitrocatechols together with 5-nitro-salicylic acid) (Lu et al., 2019a), and vehicle exhaust (dominated by 4-nitrophenol, 2,4-dinitrophenol, and 4-methyl-2,6-dinitrophenol) (Lu et al., 2019b).

During the dust event, a clear increase in concentration of nitrated phenols occurred in coarse-mode particles (3.2–5.6 μm) when compared with the normal samples. The enhancement of nitrated phenols in the coarse-mode particles was ascribed to the vast surface areas provided by dust, which facilitated the heterogeneous formation of these species on coarse particles (Wang et al., 2013a). The promoted formation of secondary components in coarse particles during dust events was also observed for sulfates and oxalates in our previous study at Mount Heng (Wang et al., 2013b). In addition, a big concentration peak was observed in droplet-mode particles (0.56–1.0 μm), possibly owing to the relatively high humidity after the dust event.

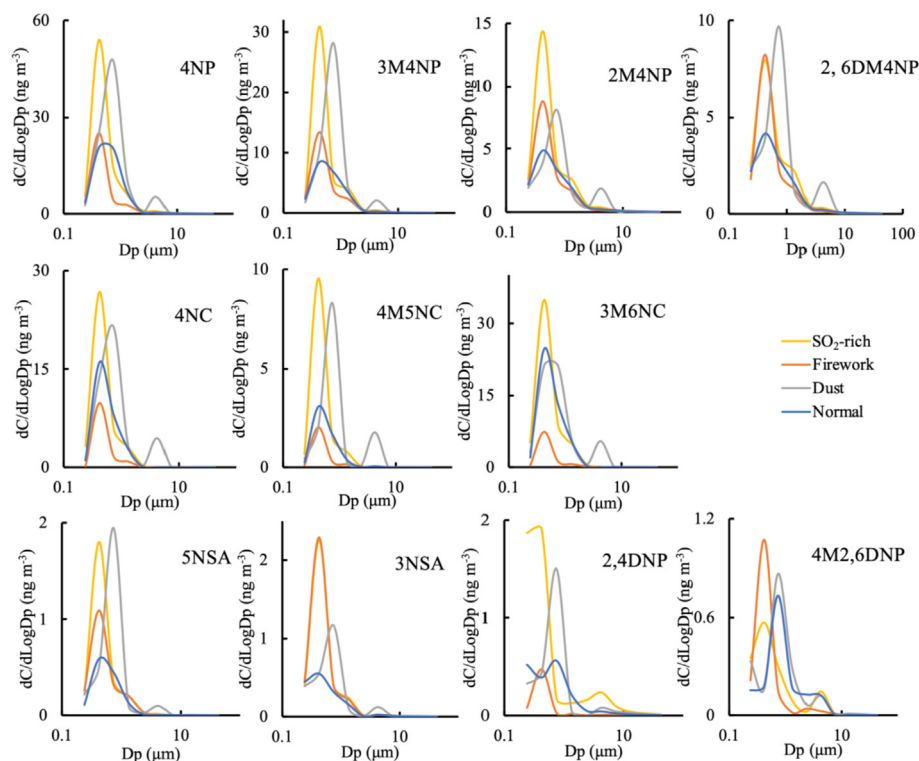


Fig. 5. Size distribution of nitrated phenols on SO₂-rich days, during a firework event, during a dust event, and on normal days.

3.4. Changes in size distributions caused by moisture and aqueous reactions

The time series plots shown in Fig. 2 demonstrate that the concentrations of particulate nitrated phenols were high under high humidity. To clarify the effect of humidity on the formation and particle size distribution of nitrated phenols, the size distributions of the 11 nitrated phenols at three humidity levels, i.e., low humidity: 49% < RH < 60%, moderate humidity: 60% < RH < 70%, and high humidity: 70% < RH < 94%, were compared, as shown in Fig. 6.

As shown in the figure, with an increase in ambient humidity, the particle size where maximum concentrations of nitrated phenols appeared changed from condensation mode to droplet mode. Specifically, at relatively low relative humidity (<60%), most nitrated phenols showed a sharp concentration peak in condensation-mode particles (0.32–0.56 μm). In moderate humidity (60% < RH < 70%), the big concentration peak of nitrated phenols shifted from the condensation mode to the droplet mode (0.56–1.0 μm). When the relative humidity exceeded 70%, the concentrations of nitrated phenols in the size ranges of 0.32–0.56 μm and 0.56–1.0 μm decreased, and a noticeable concentration peak was present in larger-size droplet-mode particles (1.0–1.8 μm), particularly of 4-nitrophenol, methyl-nitrophenols, and nitro salicylic acids. Notably, the concentrations of nitro-salicylic acids under high humidity were substantially higher than those at low and moderate humidity.

The sharp increase in the concentrations of nitrated phenols in droplet-mode particles under high humidity indicates the rapid formation of nitrated phenols by aqueous reactions in the liquid layer on the aerosol surface or within small droplets. As the relative humidity exceeded 60%, the hygroscopic substances in the fine particles likely absorbed water vapor and formed liquid water on the surfaces, which facilitated the secondary formation of nitrated

phenols through aqueous processes, similar to the aqueous-phase formation of sulfates (Fang et al., 2019; Wang et al., 2012). In the aqueous phase, nitration of phenolic precursors in the presence of N₂O₅ can form nitrated phenols (Harrison et al., 2005), and it seems that this phenomenon led to the large increase in the concentration of nitrated phenols observed in droplet-mode particles. The uptake of gaseous nitrated phenols in liquid water on aerosol surfaces may also have contributed to the increase in their concentrations in droplet-mode particles under high humidity.

In addition, a small concentration peak in coarse-mode particles (3.2–5.6 μm) was noticed for nitrocatechols, nitrophenols, and di-nitrophenols in the medium-humidity samples. This was attributable to the fact that these samples included one sample that was influenced by the dust event. The increase in crustal dusts in coarse-mode particles facilitated the formation of particulate nitrated phenols in these particles. In addition, a small concentration peak also occurred in coarse-mode particles for 4M2,6DNP (but not other nitrated phenols) in the low- and high-humidity samples. The detailed reasons for this remain unclear and require further investigation.

4. Conclusions

Eleven particulate nitrated phenols in nine size ranges were examined to investigate their size-distribution characteristics and the key influencing factors in winter at a coastal site in rural Qingdao. The concentrations of particulate nitrated phenols in winter in rural Qingdao were substantially higher than those in other locations, with the average total concentrations in fine and coarse particles of 123.6 and 27.1 ng m⁻³, respectively. Among the detected 11 nitrated phenols, 4-nitrophenol, 3-methyl-6-nitrocatechol, 3-methyl-4-nitrophenol, and 4-nitrocatechol were found to be the most abundant species. Further, it was found that both primary emission sources and secondary formation had great

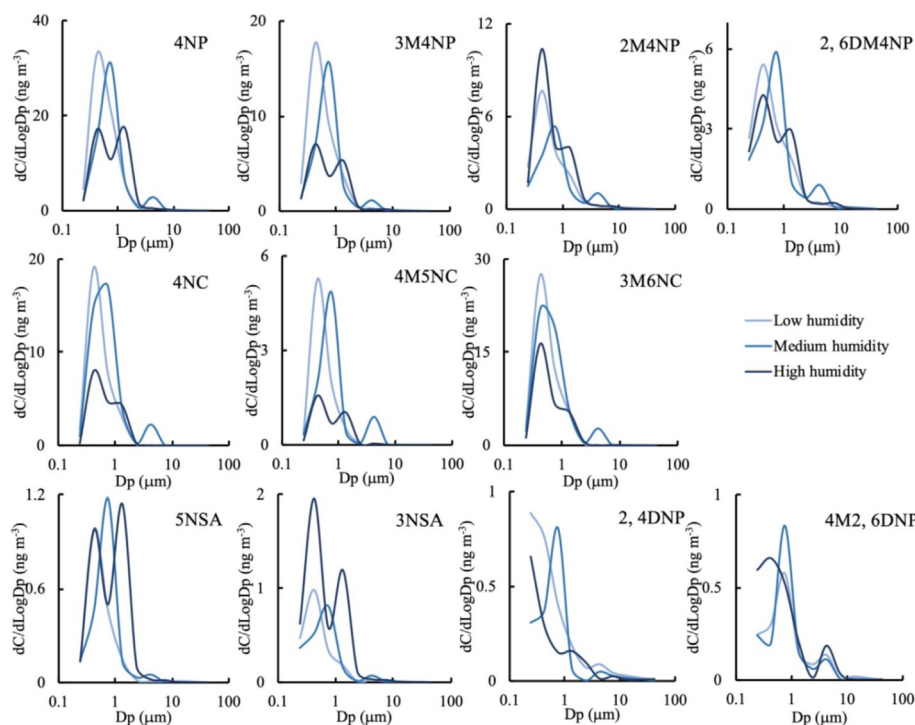


Fig. 6. Size distribution of nitrated phenols at different humidity levels.

impacts on the abundances and particle size distribution of nitrated phenols. Specifically, residential coal combustion caused a sharp increase in the concentrations of 4-nitrophenol, 4-nitrocatechol, methyl-nitrocatechols, and 2,4-dinitrophenol in condensation-mode particles, whereas firework burning during Lantern Festival celebrations led to a sharp increase in the concentrations of methyl-nitrophenols, nitro-salicylic acids, and dinitrophenols in the condensation mode. However, the presence of dust promoted the heterogeneous formation of most nitrated phenols in coarse particles. In addition, the relative humidity in the coastal area facilitated the formation of nitrated phenols in droplet-mode particles via aqueous reactions in the liquid water on particles or within small droplets.

Author contributions

Yiheng Liang collected the size-resolved samples, determined the contents of nitrated phenols, performed the data analysis, and drafted the manuscript. Xinfeng Wang designed and guided the study and revised the manuscript. Shuwei Dong provided help in sample collection. Zhiyi Liu provided help in sample treatment. Jiangshan Mu performed the online measurements of trace gases and PM_{2.5}. Chunying Lu provided the extraction and analysis methods of particulate nitrated phenols. Jun Zhang and Min Li provided help for the determination of nitrated phenol. Likun Xue and Wenxing Wang provided the analyzers for trace gases and PM_{2.5} and the sampler of MOUDI.

Credit author statement

Yiheng Liang: Validation, Formal analysis, Investigation, Data curation, Writing-Original draft. **Xinfeng Wang:** Conceptualization, Methodology, Resources, Writing-Review & editing, Supervision, Project administration, Funding acquisition. **Shuwei Dong:** Investigation. **Zhiyi Liu:** Investigation. **Jiangshan Mu:** Data curation.

Chunying Lu: Methodology. **Jun Zhang:** Investigation. **Min Li:** Investigation. **Likun Xue:** Resources. **Wenxing Wang:** Resources.

Declaration of competing interest

The authors declare that there is no conflict of interests.

Acknowledgements

This work was supported by the National Key Research and Development Program of China (no. 2016YFC0200500) and the National Natural Science Foundation of China (nos. 41775118, 91544213, and 91644214) and received financial support from Shandong University (grant no. 2020QNT012). We also appreciate the website of Weather Underground and China National Environmental Monitoring Centre for providing the data of meteorological parameters and PM_{2.5} concentrations.

References

- Andreozzi, R., Canterino, M., Caprio, V., Di Somma, I., Sanchirico, R., 2006. Salicylic acid nitration by means of nitric acid/acetic acid system: chemical and kinetic characterization. *Org. Process Res. Dev.* 10, 1199–1204.
- Attri, A.K., Kumar, U., Jain, V., 2001. Microclimate: formation of ozone by fireworks. *Nature* 411, 1015.
- Chim, M.M., Cheng, C.T., Davies, J.F., Berkemeier, T., Shiraiwa, M., Zuend, A., Chan, M.N., 2017. Compositional evolution of particle-phase reaction products and water in the heterogeneous OH oxidation of model aqueous organic aerosols. *Atmos. Chem. Phys.* 17, 14415–14431.
- Chow, K.S., Huang, X.H., Yu, J.Z., 2016. Quantification of nitroaromatic compounds in atmospheric fine particulate matter in Hong Kong over 3 years: field measurement evidence for secondary formation derived from biomass burning emissions. *Environ. Chem.* 13, 665–673.
- Cloud, 2019. IBM [Online] Available: <https://www.wunderground.com>. (Accessed 25 February 2019).
- Desyaterik, Y., Sun, Y., Shen, X., Lee, T., Wang, X., Wang, T., Collett, J.L., 2013. Speciation of “brown” carbon in cloud water impacted by agricultural biomass burning in eastern China. *J. Geophys. Res.: Atmosphere* 118, 7389–7399.
- Drewnick, F., Hings, S.S., Curtius, J., Erdekens, G., Williams, J., 2006. Measurement of fine particulate and gas-phase species during the New Year’s fireworks 2005

- in Mainz, Germany. *Atmos. Environ.* 40, 4316–4327.
- Fang, Y., Ye, C., Wang, J., Wu, Y., Hu, M., Lin, W., Xu, F., Zhu, T., 2019. Relative humidity and O₃ concentration as two prerequisites for sulfate formation. *Atmos. Chem. Phys.* 19, 12295–12307.
- Finewax, Z., de Gouw, J.A., Ziemann, P.J., 2018. Identification and quantification of 4-nitrocatechol formed from OH and NO₃ radical-initiated reactions of catechol in air in the presence of NO_x: implications for secondary organic aerosol formation from biomass burning. *Environ. Sci. Technol.* 52, 1981–1989.
- Frka, S., Sala, M., Kroflic, A., Hus, M., Cusak, A., Grgic, I., 2016. Quantum chemical calculations resolved identification of methyl-nitrocatechols in atmospheric aerosols. *Environ. Sci. Technol.* 50, 5526–5535.
- Harrison, M.A., Barra, S., Borghesi, D., Vione, D., Arsene, C., Olariu, R.I., 2005. Nitrated phenols in the atmosphere: a review. *Atmos. Environ.* 39, 231–248.
- Hofmann, D., Hartmann, F., Herrmann, H., 2008. Analysis of nitrophenols in cloud water with a miniaturized light-phase rotary perforator and HPLC-MS. *Anal. Bioanal. Chem.* 391, 161–169.
- Huang, X.F., Dai, J., Zhu, Q., Yu, K., Du, K., 2019. Abundant biogenic oxygenated organic aerosol in atmospheric coarse particles: plausible sources and atmospheric implications. *Environ. Sci. Technol.* 54, 1425–1430.
- Iinuma, Y., Böge, O., Gräfe, R., Herrmann, H., 2010. Methyl-nitrocatechols: atmospheric tracer compounds for biomass burning secondary organic aerosols. *Environ. Sci. Technol.* 44, 8453–8459.
- Jenkin, M., Saunders, S., Wagner, V., Pilling, M., 2003. Protocol for the development of the Master Chemical Mechanism, MCM v3 (Part B): tropospheric degradation of aromatic volatile organic compounds. *Atmos. Chem. Phys.* 3, 181–193.
- Kahnt, A., Behrouzi, S., Vermeylen, R., Shalamzari, M.S., Vercauteren, J., Roekens, E., Claeys, M., Maenhaut, W., 2013. One-year study of nitro-organic compounds and their relation to wood burning in PM₁₀ aerosol from a rural site in Belgium. *Atmos. Environ.* 81, 561–568.
- Kitanovski, Z., Grgić, I., Vermeylen, R., Claeys, M., Maenhaut, W., 2012. Liquid chromatography tandem mass spectrometry method for characterization of monoaromatic nitro-compounds in atmospheric particulate matter. *J. Chromatogr. A* 1268, 35–43.
- Köhler, M., Heeb, N.V., 2003. Determination of nitrated phenolic compounds in rain by liquid chromatography/atmospheric pressure chemical ionization mass spectrometry. *Anal. Chem.* 75, 3115–3121.
- Kowalczyk, A., Eyice, Ö., Schäfer, H., Price, O.R., Finnegan, C.J., van Egmond, R.A., Shaw, L.J., Barrett, G., Bending, G.D., 2015. Characterization of para-nitrophenol-degrading bacterial communities in river water by using functional markers and stable isotope probing. *Appl. Environ. Microbiol.* 81, 6890–6900.
- Laskin, A., Laskin, J., Nizkorodov, S.A., 2015. Chemistry of atmospheric brown carbon. *Chem. Rev.* 115, 4335–4382.
- Li, J., Wang, G., Zhou, B., Cheng, C., Cao, J., Shen, Z., An, Z., 2011. Chemical composition and size distribution of wintertime aerosols in the atmosphere of Mt. Hua in central China. *Atmos. Environ.* 45, 1251–1258.
- Li, X., Jiang, L., Lyu, Y., Xu, T., Yang, X., Iinuma, Y., Chen, J., Herrmann, H., 2016. Size distribution of particle-phase sugar and nitrophenol tracers during severe urban haze episodes in Shanghai. *Atmos. Environ.* 145, 115–127.
- Lu, C., Wang, X., Dong, S., Zhang, J., Li, J., Zhao, Y., Liang, Y., Xue, L., Xie, H., Zhang, Q., 2019b. Emissions of fine particulate nitrated phenols from various on-road vehicles in China. *Environ. Res.* 179, 108709.
- Lu, C., Wang, X., Li, R., Gu, R., Zhang, Y., Li, W., Gao, R., Chen, B., Xue, L., Wang, W., 2019a. Emissions of fine particulate nitrated phenols from residential coal combustion in China. *Atmos. Environ.* 203, 10–17.
- Luo, C., Zender, C.S., Bian, H., Metzger, S., 2007. Role of ammonia chemistry and coarse mode aerosols in global climatological inorganic aerosol distributions. *Atmos. Environ.* 41, 2510–2533.
- Mohr, C., Lopez-Hilfiker, F.D., Zotter, P., Prévôt, A.S., Xu, L., Ng, N.L., Herndon, S.C., Williams, L.R., Franklin, J.P., Zahniser, M.S., 2013. Contribution of nitrated phenols to wood burning brown carbon light absorption in Detling, United Kingdom during winter time. *Environ. Sci. Technol.* 47, 6316–6324.
- Rubio, M.A., Lissi, E., Herrera, N., Pérez, V., Fuentes, N., 2012. Phenol and nitrophenols in the air and dew waters of Santiago de Chile. *Chemosphere* 86, 1035–1039.
- Saccon, M., Facca, C., Huang, L., Irei, S., Kornilova, A., Lane, D., Rudolph, J., 2013. Method for the determination of concentration and stable carbon isotope ratios of atmospheric phenols. *Atmos. Meas. Tech.* 6, 2965–2974.
- Schummer, C., Groff, C., Al Chami, J., Jaber, F., Millet, M., 2009. Analysis of phenols and nitrophenols in rainwater collected simultaneously on an urban and rural site in east of France. *Sci. Total Environ.* 407, 5637–5643.
- Shchekin, A.K., Podguzova, T.S., 2011. The modified Thomson equation in the theory of heterogeneous vapor nucleation on charged solid particles. *Atmos. Res.* 101, 493–502.
- Teich, M., van Pinxteren, D., Wang, M., Kecorius, S., Wang, Z., Müller, T., Močnik, G., Herrmann, H., 2017. Contributions of nitrated aromatic compounds to the light absorption of water-soluble and particulate brown carbon in different atmospheric environments in Germany and China. *Atmos. Chem. Phys.* 17, 1653–1672.
- Vione, D., Maurino, V., Minero, C., Pelizzetti, E., 2005. Aqueous atmospheric chemistry: formation of 2,4-dinitrophenol upon nitration of 2-nitrophenol and 4-nitrophenol in solution. *Environ. Sci. Technol.* 39, 7921–7931.
- Wang, L., Wang, X., Gu, R., Wang, H., Yao, L., Wen, L., Zhu, F., Wang, W., Xue, L., Yang, L., 2018a. Observations of fine particulate nitrated phenols in four sites in northern China: concentrations, source apportionment, and secondary formation. *Atmos. Chem. Phys.* 18, 4349–4359.
- Wang, H., Lu, K., Guo, S., Wu, Z., Shang, D., Tan, Z., Wang, Y., Breton, M.L., Lou, S., Tang, M., 2018b. Efficient N₂O₅ uptake and NO₃ oxidation in the outflow of urban Beijing. *Atmos. Chem. Phys.* 18, 9705–9721.
- Wang, X., Wang, W., Xue, L., Gao, X., Nie, W., Yu, Y., Zhou, Y., Yang, L., Zhang, Q., Wang, T., 2013b. Size-resolved aerosol ionic composition and secondary formation at Mount Heng in South Central China. *Front. Environ. Sci. Eng.* 7, 815–826.
- Wang, X., Wang, W., Yang, L., Gao, X., Nie, W., Yu, Y., Xu, P., Zhou, Y., Wang, Z., 2012. The secondary formation of inorganic aerosols in the droplet mode through heterogeneous aqueous reactions under haze conditions. *Atmos. Environ.* 63, 68–76.
- Wang, G., Zhou, B., Cheng, C., Cao, J., Li, J., Meng, J., Tao, J., Zhang, R., Fu, P., 2013a. Impact of Gobi desert dust on aerosol chemistry of Xi'an, inland China during spring 2009: differences in composition and size distribution between the urban ground surface and the mountain atmosphere. *Atmos. Chem. Phys.* 13.
- Wang, H., Zhu, B., Shen, L., Zhang, Z., Liu, X., 2014. The mass concentration and chemical compositions of the atmospheric aerosol during the Spring Festival in Nanjing. *J. Environ. Sci. (China)* 34, 30–39.
- Wang, X., Gu, R., Wang, L., Xu, W., Zhang, Y., Chen, B., Li, W., Xue, L., Chen, J., Wang, W., 2017. Emissions of fine particulate nitrated phenols from the burning of five common types of biomass. *Environ. Pollut.* 230, 405–412.
- Wang, Y., Hu, M., Wang, Y., Zheng, J., Shang, D., Yang, Y., Liu, Y., Li, X., Tang, R., Zhu, W., 2019. The formation of nitro-aromatic compounds under high NO_x and anthropogenic VOC conditions in urban Beijing, China. *Atmos. Chem. Phys.* 19, 7649–7665.
- Yan, J., Wang, X., Gong, P., Wang, C., Cong, Z., 2018. Review of brown carbon aerosols: recent progress and perspectives. *Sci. Total Environ.* 634, 1475–1485.
- Yuan, B., Liggio, J., Wentzell, J., Li, S.M., Stark, H., Roberts, J.M., Gilman, J., Lerner, B., Warneke, C., Li, R., 2016. Secondary formation of nitrated phenols: insights from observations during the Uintah basin winter ozone study (UBWOS) 2014. *Atmos. Chem. Phys.* 16, 2139–2153.
- Zhang, D., Zang, J., Shi, G., Iwasaka, Y., Matsuki, A., Trochke, D., 2003. Mixture state of individual Asian dust particles at a coastal site of Qingdao, China. *Atmos. Environ.* 37, 3895–3901.
- Zhang, Y., Müller, L., Winterhalter, R., Moortgat, G., Hoffmann, T., Pöschl, U., 2010. Seasonal cycle and temperature dependence of pinene oxidation products, dicarboxylic acids and nitrophenols in fine and coarse air particulate matter. *Atmos. Chem. Phys.* 10, 7859–7873.
- Zhang, Z., Zhu, T., Shang, J., Zhao, D., Ye, C., 2011. Heterogeneous reaction of NO₂ on the surface of kaolinite particles. *Acta Sci. Circumstantiae* 31, 2073–2079.